Design of Orthogonal Coded Excitation for Synthetic Aperture Imaging in Ultrasound Systems*

Ming Yang and Chaitali Chakrabarti
School of Electrical, Computer and Energy Engineering
Arizona State University, Tempe, Arizona
email: m.yang@asu.edu, chaitali@asu.edu

Abstract— **This paper presents a new digital front-end architecture for synthetic aperture ultrasound (SAU) imaging using orthogonal chirps and orthogonal Golay codes. Compared to existing systems that perform decoding before beamforming, the proposed systems have comparable performance and significantly lower computation and space complexity. Unfortunately the proposed systems suffer loss in performance in the presence of body motion. To address this problem, we propose a simple motion compensation scheme that improves both the SNR and the RSLL performance. A comparison of the complexity of both the systems shows that while Golay code-based system has lower computation complexity than chirp-based system, if motion compensation is included, then the complexity of the two systems are comparable.**

I. Introduction

Synthetic aperture imaging (SAU) is a popular imaging mode that has been used in ultrasound systems for the past few decades. It can support very high frame rates compared to phased array imaging, since its frame rate does not depend on the number of scanlines. It also has better resolution since its beamforming is equivalent to performing dynamic focusing on both transmit and receive ends. Unfortunately, traditional SAU systems suffer from low signal-to-noise (SNR) and low contrast. Temporal coded excitation using chirps and Golay codes have large time-bandwidth product and can improve the SNR of SAU systems though only by about 15dB [1]. Orthogonal coding in spatial domain can further improve the SNR by typically 10~20dB as shown in [2]–[4].

There exist several coded excitation systems based on orthogonal Golay codes and chirps [2]–[4]. In these systems, the RF-data from the A/D converter is first decoded using a Hadamard transform. This data is then processed by a compression filter in case of a chirp-based system or two code correlators in case of a Golay code-based system. The decoded data is then sent to a beamformer. We define such a system as decoding-first since the decoding is done before beamforming. While such a system has the advantage of simple beamforming, it results in high computation and storage complexity. Moreover SAU systems with orthogonal codes are sensitive to body motion and in the decoding-first architecture, the motion artifacts can not be easily compensated.

In this paper, we present an efficient architecture for orthogonal chirp and orthogonal Golay code-based systems that integrates decoding with beamforming. The proposed architecture significantly reduces computation complexity and storage space compared to existing decoding-first systems. We compare the performance of the two proposed systems in presence of motion and propose a simple motion compensation scheme which can significantly improve the system performance in terms of SNR and range sidelobe level (RSLL). We compare the implementation complexity of both systems and show that while orthogonal Golay code-based system has lower computation complexity compared to chirp-based system, when motion compensation is included, both systems have comparable complexity.

The rest of the paper is organized as follows. Section II gives an overview of the proposed decoding and beamforming architecture along with a comparison of the implementation complexity of orthogonal chirp and orthogonal Golay code based SAU systems. In section III, the performance of the candidate systems in the presence of motion is compared. In Section IV, a motion compensation method is proposed and the corresponding performance is presented. The paper is concluded in Section V.

II. Algorithm Overview

In the decoding-first system, each of the N channels stores M sets of signals corresponding to M transmissions. Then Hadamard transform is used to decode the data in each channel. After spatial decoding, the signal streams corresponding to each transmit-receive pair are separated and processed by a compression filter in case of chirp-based system or code correlators in case of Golay code-based system. The data is interpolated to increase the sampling rate and then sent to the beamforming unit.

The advantage of this system is that all the addition processing is done before beamforming, and so the beamforming architecture of traditional SAU systems can be used. The disadvantage is that it needs to buffer multiple subframes, which increases space complexity. Moreover, for each pair of transmit-receive elements, correlation or compression filtering has to be performed, resulting in high computation complexity. Also, the architecture cannot be easily extended to incorporate motion compensation. This is because the signals received in different transmissions are summed up during decoding and so the delay cannot be adjusted during beamforming.

* This work was funded in part by grant NSF-CSR0910699.

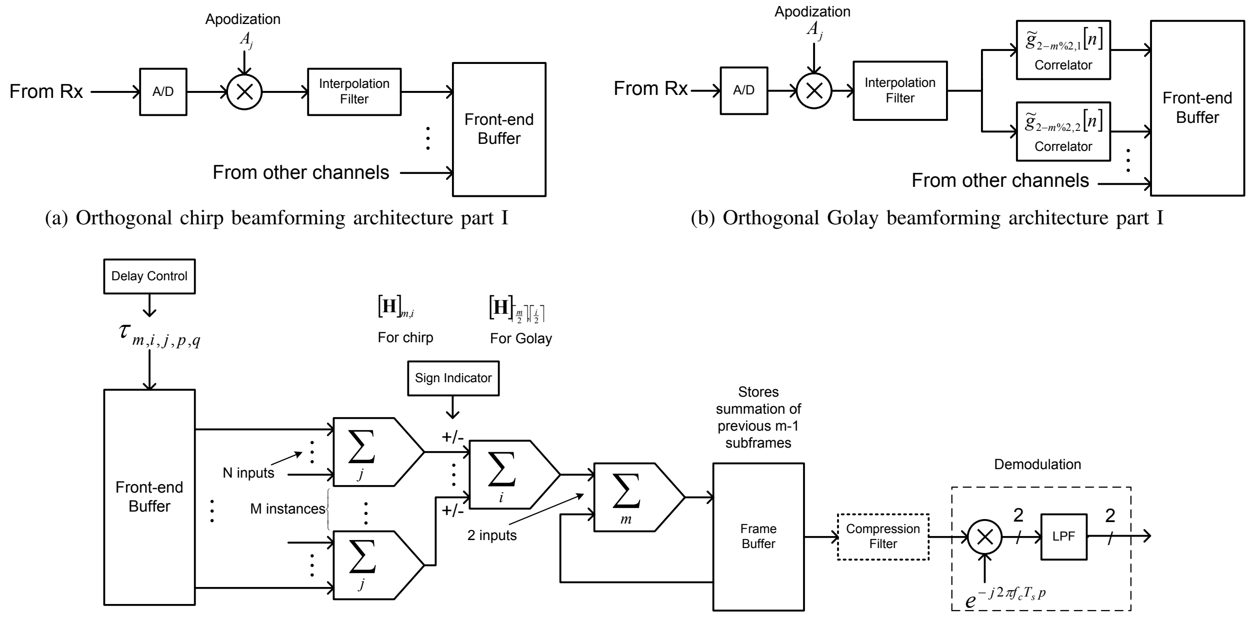

(a) Orthogonal chirp beamforming architecture part I

(b) Orthogonal Golay beamforming architecture part I

(c) Beamforming part II

Fig. 1: Beamforming architectures for orthogonal Golay and chirp with demodulation after beamforming

Next we propose a new architecture which integrates decoding with beamforming. The proposed architecture has comparable performance and significantly lower computation and storage complexity compared to the decoding-first system.

A. Proposed beamforming architecture

The proposed digital front-end architectures for orthogonal chirp and orthogonal Golay based systems corresponding to one receive chain are shown in Fig.1a and Fig.1b, respectively. The first unit is apodization, which is a fixed-coefficient spatial window that can reduce lateral sidelobe levels. Next, interpolation filtering is done to increase the sampling rate from 40MHz at the A/D to 120MHz. For the Golay code-based system, two correlators are used to generate two versions of correlated signals for decoding. The output of the interpolation filter in case of chirp-based system or the output of the two correlators in case of Golay code-based system, is stored in the front-end buffer for further processing by the beamforming unit.

The beamforming architecture, shown in Fig.1c, is almost the same for Golay code and chirp-based systems. The delay control unit chooses the signal samples from the front-end buffer according to delay $\tau_{m,i,j,p,q}$, where m is the transmission index, i is the transmit (Tx) element index, j is the receive (Rx) element index, p is the focal point index and q is the scanline index. Clearly, τ is a function of i, j, p and q, and in presence of motion, it is also a function of m.

There are three stages of summation. The first stage, which consists of M summers, sums signal samples from N receiving elements. In the second stage, the signal samples corresponding to M transmit elements are summed up, thereby generating the value corresponding to a focal point. The Hadamard matrices $\mathbf{H}_{M\times M}$ for chirp-based system and $\mathbf{H}_{\frac{M}{2}\times\frac{M}{2}}$ for Golay code-based system are used to decide whether to add or subtract the streams corresponding to different transmit elements. For example, if $[\mathbf{H}]_{\lceil\frac{m}{2}\rceil,\lceil\frac{i}{2}\rceil} = -1$ in a Golay code-based system, the stream corresponding to the mth transmission from the ith element is subtracted from the streams from the mth transmission of all the other transmit elements. Actually this stage merges the spatial decoding and beamforming together. For the mth transmission, this process is repeated PQ times and an image containing PQ focal points for the mth transmission is generated. In the third stage, the image frame stored in the frame buffer is updated with the one generated in the mth transmission.

The data in the frame buffer is then demodulated. In case of a chirp-based system, there is a compression filter before the demodulation stage. Both compression filtering and demodulation are done scanline by scanline.

B. Implementation Complexity

The complexity of the Golay code-based and chirp-based systems are compared using the parameters defined in Table I. While the Golay code-based system requires two correlation units, they involve only additions and subtractions. The chirp-based system, on the other hand, requires a compression filter which increase the complexity significantly – about $PQT_{code}f_s$ additional multiplications per image. For the setting in Table I, the chirp-based system needs about 1.1×10^{10} multiplications per image, while the Golay code-based system needs only 2.9×10^{8} multiplications.

A comparison of the complexity of the proposed chirp-based system and the chirp-based system implemented with decoding-first scheme shows that the proposed system requires

TABLE I: Parameter definitions and values

Symbol	Description	Value
N	Number of receiving elements	128
M	Number of transmitting elements and number of transmissions	32
f_c	Transducer central frequency	4 MHz
B	6dB bandwidth of transducer	4 MHz
f_s	A/D sampling frequency	40 MHz
f'_s	Sampling frequency after interpolation	120 MHz
T_{code}	Duration of the coded excitation	32 μs
K_{LPF}	Number of taps of demodulation lowpass filter	36
K_{INT}	Number of taps of interpolation lowpass filter	5
D	Maximum detection depth	20 cm
c	Speed of sound in body tissue	1540 m/s
P	Number of focal points in one scanline	1.04×10^4
Q	Number of scanline in one image	200

significantly fewer multiplications, $PQT_{code}f_s$ compared to $PMNT_{code}f_s$. Thus for the setting in Table I, the proposed chirp-based system needs only ~5% of the multiplications required by the corresponding decoding-first system. In terms of space complexity, the decoding-first architecture has to buffer all M subframes received in M transmissions. In contrast, the proposed architecture only needs to buffer the receive data in one subframe though this data is stored at a higher sampling rate because of interpolation. Thus, the space complexity is reduced to $\frac{f'_s}{f_s M}$ or 9.4% of decoding-first architecture for the setting in Table I.

For orthogonal Golay code-based systems proposed in [4], [5], $2M$ correlators perform N times for one image, while in the proposed system, $2N$ correlators perform M times. Hence the complexity of the two systems in terms of code correlation is the same. However in terms of space complexity, the proposed architecture only needs to buffer two correlated versions of receive data in one subframe. In contrast, the decoding-first system stores M subframes. Hence the proposed architecture only needs $\frac{2f'_s}{f_s M}$ of the storage needed by the decoding-first architecture.

III. Performance Evaluation

In this section, the performance of the two coded excitation systems are compared. All simulations are done using Field II [6], [7] using the parameters listed in Table I. Only one target at depth of 6cm is considered and the point spread function at that depth is presented.

Fig. 2 plots the SNR for different motion speeds for the Golay code and chirp-based systems. The motion speed is varied from 0 to 2 cm/s. When there is no motion (speed = 0 cm/s), the proposed chirp-based system has about 1dB higher SNR than the corresponding decoding-first system. For Golay code-based systems, the two schemes (proposed and decoding-first) have the same performance in absence of motion.

In presence of body motion, the performance of SAU systems with orthogonal coding is degraded. This is because an SAU image is obtained by coherently combining M subframes corresponding to M transmissions. Especially, perfect sidelobe cancellation of orthogonal Golay codes rely on perfect timing and phase coherence. Chirps are less sensitive in terms of sidelobe levels, but if the phase coherence is lost due to body motion, the SNR of the image is affected as well. Fig. 2 shows that in presence of motion the SNR drops in all the systems. Compared to Golay code-based systems, chirp-based systems have higher SNR drop as motion speed increases. The architectures based on decoding-first system suffer even higher SNR loss.

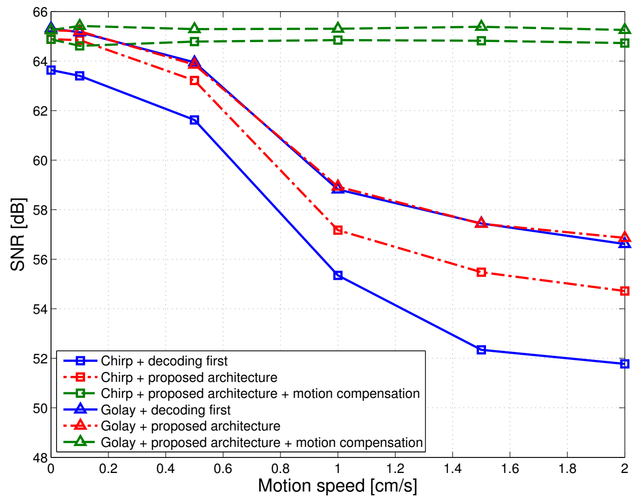

Fig. 2: SNR vs. motion speed

Next, we present the RSLL curves versus motion speed in Fig. 3. The RSLL of Golay code-based system is higher than -50dB when speed is larger than 0.5cm/s. In contrast, chirp-based systems have much lower RSLL in presence of motion. The chirp-based decoding-first system has the lowest RSLL compared to systems where there is no motion compensation.

In summary, although Golay code-based system is better in terms of SNR, chirp-based system is better in terms of RSLL. All SAU systems based on orthogonal codes have significant performance drop when motion speed is larger than 0.5cm/s. The motion artifacts are even more significant as the code length and number of transmit elements increases. Thus motion compensation should be considered for SAU systems that require high performance.

IV. Motion Compensation

In this section we describe a simple motion compensation scheme for the proposed architecture. The idea is that if the motion velocity can be estimated (as in [8]), then the beamforming algorithm can dynamically adjust the delay and phase correction term and the focal point can follow the moving target points [9]. Here we propose a simplified version of the method in [9] using Taylor expansion to update $\tau_{m,i,j,p,q}$, which requires only 2 multiplications for each delay value.

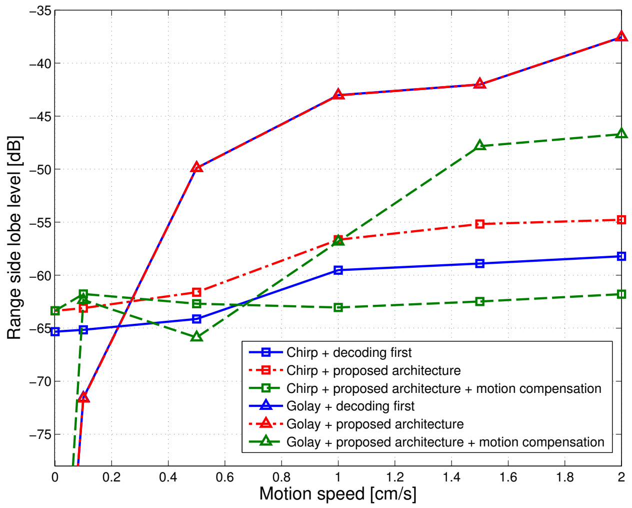

Fig. 3: Range sidelobe level vs. motion speed

In the absence of motion, the delay $\tau_{m,i,j,p,q}$ is constant for all transmissions. This can be calculated by $\tau_{m,i,j,p,q} = (A_{j,p,q} + B_{i,p,q})/c$, where $A_{j,p,q} = \sqrt{(x_j - x_{p,q})^2 + z_{p,q}^2}$ and $B_{i,p,q} = \sqrt{(x_i - x_{p,q})^2 + z_{p,q}^2}$ are the distance between the focal point and the jth Rx element and the ith Tx element, respectively. This part can be pre-calculated and stored in a look up table.

If motion artifacts are significant, then it is necessary to add a compensation value $\Delta\tau_{m,i,j,p,q}$ to the delay value of the next transmission.

$$\Delta\tau_{m,i,j,p,q} = \frac{1}{c}\left(\frac{x_{p,q} - x_j}{A_{j,p,q}} + \frac{x_{p,q} - x_i}{B_{i,p,q}}\right) v_x \Delta t + \frac{1}{c}\left(\frac{z_{p,q}}{A_{j,p,q}} + \frac{z_{p,q}}{B_{i,p,q}}\right) v_z \Delta t \quad (1)$$

where $z_{p,q}$ is the z coordinate of the focal point p in scanline q, Δt is the time interval between two transmissions. For efficient computation of $\Delta\tau_{m,i,j,p,q}$, we need two look-up tables, one to store $\frac{(x_{p,q} - x_j)\Delta t}{cA_{j,p,q}}$ and the other to store $\frac{z_{p,q}\Delta t}{cA_{j,p,q}}$. Each table has NPQ elements, which is fairly large. But in a real implementation, the symmetry of the scanlines and transducer elements and the fact that the delay will be eventually mapped to an integer memory address, is used to reduce the size of the tables.

The proposed motion compensation method is quite effective as shown in Fig. 2 and 3. For instance, Fig. 2 shows that this method can improve the SNR for both chirp-based and Golay code-based systems by as much as 10dB. After motion compensation, the difference between the performance of Golay code-based system and chirp-based system is quite small.

Fig. 3 shows how RSLL is also reduced by the motion compensation method. The chirp-based system with motion compensation reduces the RSLL to under -60dB for all simulated motion speeds, but Golay code-based system with motion compensation can not reduce it to less than -57dB when motion speed is larger than 1cm/s.

While the proposed motion compensation method is very simple, it adds significant computation complexity. For each focal point, there are now two additional multiplications, which translates to $2NM^2PQ$ multiplications for one frame. For the setting in Table I, the total number of multiplications for the chirp-based system with motion compensation is 5.56×10^{11} and for the Golay code-based system with motion compensation is 5.45×10^{11}. Thus the two coding systems have comparable computation complexity when motion compensation is included.

V. Conclusion

In this paper we first propose a new decoding and beamforming architecture for synthetic aperture ultrasound using orthogonal chirp and orthogonal Golay codes. We show that the implementation complexity of the proposed architecture is much less than existing decoding-first systems. We analyze the performance of the proposed systems in the presence of body motion and see that while both systems have degraded SNR and RSLL performance, the Golay code-based system has higher SNR and the chirp-based system has lower RSLL. Next we propose a simple motion compensation method that enhances the performance of both the systems. We also compare the computation complexity of the proposed systems and show that while the Golay code-based system is less complex than chirp-based system, if motion compensation is included, the two systems have comparable complexity.

References

[1] M. O'Donnell and Y. Wang, "Coded excitation for synthetic aperture ultrasound imaging," *IEEE Transactions on Ultrasonics, Ferroelectrics and Frequency Control*, vol. 52, no. 2, pp. 171 –176, Feb. 2005.

[2] T. Misaridis and J. Jensen, "Space–time encoding for high frame rate ultrasound imaging," *Ultrasonics*, vol. 40, no. 1, pp. 593–597, 2002.

[3] ——, "Use of modulated excitation signals in medical ultrasound. part III: high frame rate imaging," *IEEE Transactions on Ultrasonics Ferroelectrics and Frequency Control*, vol. 52, no. 2, pp. 208 –219, Feb. 2005.

[4] R. Chiao and L. Thomas, "Synthetic transmit aperture imaging using orthogonal Golay coded excitation," in *Proceedings of IEEE Ultrasonics Symposium*, vol. 2, Oct. 2000, pp. 1677 –1680.

[5] R. Chiao and L. Thomas III, "Method and apparatus for ultrasonic synthetic transmit aperture imaging using orthogonal complementary codes," Apr. 11 2000, US Patent 6,048,315.

[6] J. A. Jensen, "Field: A program for simulating ultrasound systems," in *10th Nordicbaltic Conference on Biomedical Imaging, Vol. 4, Supplement 1, Part 1:351–353*, 1996, pp. 351–353.

[7] J. Jensen and N. Svendsen, "Calculation of pressure fields from arbitrarily shaped, apodized, and excited ultrasound transducers," *IEEE Transactions on Ultrasonics Ferroelectrics and Frequency Control*, vol. 39, no. 2, pp. 262 –267, Mar 1992.

[8] F. Mauldin, F. Viola, and W. Walker, "Complex principal components for robust motion estimation," *IEEE Transactions on Ultrasonics, Ferroelectrics and Frequency Control*, vol. 57, no. 11, pp. 2437 –2449, Nov. 2010.

[9] K. G. S. Nikolov and J. Jensen, "Velocity estimation using recursive ultrasound imaging and spatially encoded signals," in *IEEE Ultrasonics Symposium 2000*, vol. 2, pp. 1473 –1477.